On the Use of the Angle of Incidence in Support Vector Regression Surrogate Models for Practical Reflectarray Design

Daniel R. Prado, Jesús A. López-Fernández, Manuel Arrebola, *Senior Member, IEEE* and George Goussetis, *Senior Member, IEEE*

***Abstract*—A common approach in the literature when obtaining surrogate models of reflectarray unit cells is to include, among other variables, the angles of incidence as input variables to the model. In this work, we use support vector regression (SVR) to compare this approach with a new strategy which consists in grouping the refletarray elements under a small set of angles of incidence and train surrogate models per angle of incidence pair. In this case, the dimensionality of the SVR decreases in two with regard to the former approach. In both cases, two geometrical variables are considered for reflectarray design, obtaining 4D and 2D SVRs, respectively. In contrast to the common approach in the literature, the comparison between the 4D and 2D SVRs shows that a proper discretization of the angles of incidence is more competitive than introducing the angles as input variables in the SVR. The 2D SVR offers a shorter training time, faster reflectarray analysis, and a similar accuracy than the 4D SVR, making it more suitable for design and optimization procedures.**

***Index Terms*—Machine learning, surrogate model, support vector regression (SVR), angle of incidence, reflectarray antenna**

I. Introduction

SURROGATE models for reflectarray analysis have been proposed to speed-up the analysis, design and optimization of this kind of antenna using different machine learning techniques (MLTs) such as artificial neural network [1]–[6], support vector machines for regression (SVR) [7] and ordinary kriging (OK) [8]. The first efforts were aimed at predicting the phase-shift of the reflectarray element [1]–[4], which corresponds to the phase of the complex direct coefficients. This is useful since this phase mainly controls the shape of the copolar far field pattern [9]. In addition, it can also be used to obtain the reflectarray layout [10]. However, an accurate prediction of the crosspolar pattern requires the characterization of the full reflection coefficient matrix [11]. Thus, later works on MLTs applied to reflectarrays have also considered the cross-coefficients [5]–[8]. An example of application in which this is critical is contoured beams for space applications, where cross-polarization requirements are very tight and the crosspolar pattern is more than 30 dB below the copolar pattern in the region of interest [10].

In the above-mentioned MLTs, the behaviour of a reflectarray unit cell is characterized by four complex numbers known as reflection coefficients. These coefficients mainly depend on the geometrical features of the unit cell, although they are also affected by frequency and the angles of incidence [12], [13]. Thus, it is common practise to consider one or more geometrical features, the angle of incidence and frequency as input parameters to the MLT [2], [3], [8]. However, in order to keep a constant sampling density the number of training samples grows exponentially with the number of input space dimensions. As a consequence, the higher the dimensionality of the input space, the greater the workload to obtain the surrogate model.

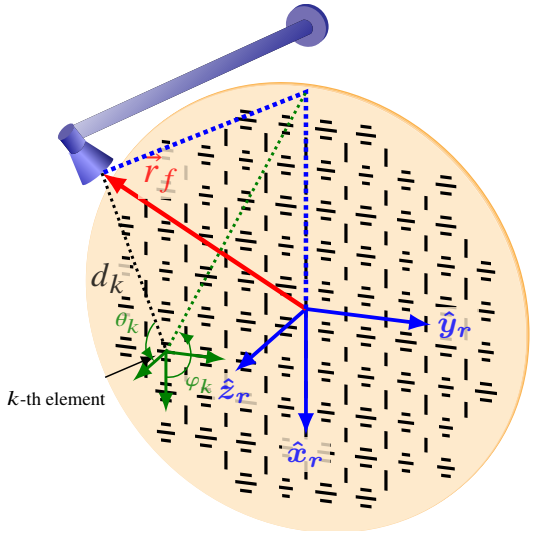

Fig. 1. Sketch of a single-offset reflectarray configuration.

Dimensionality may be reduced by training one surrogate model per incidence angle (θ, φ). In this way, the dimensionality is reduced by two dimensions, potentially improving performance of the MLT. However, each reflectarray element experiences a different angle of incidence, and having one model per reflectarray element may deem ineffective the time savings from the reduced dimensionality. Instead, the number of models may be reduced by grouping a number of reflectarray elements under the same angle of incidence. This was the strategy followed in [7], [10]. Nevertheless, there exists no study in the literature that compares these different approaches with regard to angles of incidence: including them as input variables in the model, or generating one model per considered angle of incidence. Currently, it is a question open to debate in the community which approach is more interesting to use.

In this work, a systematic study comparing the two methodologies concerning the use of angles of incidence in surrogate models with SVR is presented. Two geometrical features of a reflectarray unit cell are used as input variables of the SVR in both cases, thus obtaining a 4D SVR model when the angles of incidence are also considered as input variables, and a 2D SVR model per angle of incidence. In both cases, the training process is based on cross-validation to find the optimum model. A 2D SVR model is compared with the 4D SVR at

This work was supported in part by the European Commission under H2020 project REVOLVE (MSCA-ITN-2016-722840); by the Ministerio de Ciencia, Innovación y Universidades under projects TEC2017-86619-R (ARTEINE) and IJC2018-035696-I; by the Ministerio de Economía, Industria y Competitividad under project TEC2016-75103-C2-1-R (MYRADA); by the Gobierno del Principado de Asturias/FEDER under Project GRUPIN-IDI/2018/000191; by Ministerio de Educación, Cultura y Deporte / Programa de Movilidad "Salvador de Madariaga" (Ref. PRX18/00424).

D. R. Prado, J. A. López-Fernández and M. Arrebola are with the Department of Electrical Engineering, Group of Signal Theory and Communications, Universidad de Oviedo, Gijón, Spain (e-mail: drprado@uniovi.es; jelofer@uniovi.es; arrebola@uniovi.es).

G. Goussetis is with the Institute of Sensors, Signals and Systems, School of Engineering and Physical Sciences, Heriot-Watt University, Edinburgh, U.K. (email: g.goussetis@hw.ac.uk).

Color versions of one or more of the figures in this paper are available online at http://ieeexplore.ieee.org.

both the surrogate model level and the antenna level (by evaluating different radiation patterns). This comparison comprises two aspects: accuracy and computational efficiency. In all instances, the errors are computed with regard to the reference simulations provided by a full-wave analysis tool based on local periodicity (FW-LP) employed to generate the electromagnetic samples and analyse the reflectarray.

II. Problem Statement

A. Introduction

For reflectarray antennas, the final goal of employing surrogate models is to predict the electromagnetic response of the unit cell for a fast and accurate analysis of the antenna. In this work, the single-offset configuration shown in Fig. 1 is considered. The antenna is comprised of a flat panel with an array of K reflecting elements which are characterized by the matrix of reflection coefficients:

$$\boldsymbol{R}_k = \begin{pmatrix} \rho_{xx,k} & \rho_{xy,k} \\ \rho_{yx,k} & \rho_{yy,k} \end{pmatrix} \tag{1}$$

with $k = 1, 2, \ldots, K$. In (1), ρ_{xx} and ρ_{yy} are known as the direct coefficients and control the shape of the copolar pattern. ρ_{xy} and ρ_{yx} are the cross-coefficients and they represent an important contribution to the crosspolar pattern. Thus, a correct characterization of the complete radiation pattern requires to model the full reflection coefficient matrix. The reflection coefficients are complex numbers and they are computed with a FW-LP [9], [12]. A correct computation takes into account the geometrical features of the cell, substrate characteristics, periodicity, frequency, and angle of incidence (which is defined for the $k-$th element in Fig. 1). From these parameters, the most important are the geometrical features, since they allow to perform array design to obtain a certain copolar pattern. The periodicity and substrate are usually fixed beforehand.

The importance of using the real angle of incidence at each element for reflectarray analysis has been known for many years and used in the design of reflectarrays [12], [13]. On the one hand, the copolar pattern is not very sensitive to the angle of incidence thanks to the angular stability of the direct coefficients. This is the reason why it is possible to achieve copolar designs using the normal incidence curve [14]–[16]. On the other hand, the cross-coefficients exhibit a highly non-linear behaviour with the angle of incidence which motivates the use of a good approximation of the real angle of incidence for the analysis of the crosspolar pattern. This general behaviour is expected for common reflectarray unit cells in the literature.

In light of the previous considerations, we analyse two approaches to include the angle of incidence in surrogate models for reflectarray unit cells. In the first approach, two geometric features of the unit cell (noted as T_x and T_y) along with θ and φ are considered as input variables to the model. These variables may be grouped into a 4D input vector $\vec{x} = (T_x, T_y, \theta, \varphi)$ which is used to produce a single 4D SVR model that characterises each component of the reflection coefficients in (1). In the second approach, the input vector is formed as $\vec{x} = (T_x, T_y)$. Thus, one 2D SVR model should be produced per considered angle of incidence to characterise the reflection coefficients.

B. Surrogate Modelling Based on SVR

The basic SVR theory applied to reflectarray analysis and the training strategy employed in this work can be both consulted in [7]. Here we will review some basic concepts and define the errors which will be used in later Sections to compare the different models.

In the problem at hand, the training procedure uses a set comprised of N inputs ($\vec{x}_i \in \chi \subseteq \mathbb{R}^L$) and outputs ($\rho_i \in \mathbb{R}$, where ρ_i denotes the real part, imaginary part or magnitude of the reflection coefficients), $T = \{\vec{x}_i, \rho_i\}_{i=1,2,...,N}$, to obtain a function f that estimates the value of ρ, corresponding to any new input $\vec{x} \in \chi$. Here, the selection of the optimal SVR model follows an efficient grid search in addition to a cross-validation procedure, as detailed in [7]. This is accomplished by dividing the whole data set into three disjoint subsets: training ($N_r \leq 0.7N$), validation ($N_v = 0.15N$), and test ($N_t = 0.15N$).

In addition, we use the following definition of the relative error to measure the accuracy of the model:

$$\mathrm{RE}_{\mathrm{SVR}} = 20 \log_{10} \left(\frac{\|\vec{e}\|}{\|\vec{\rho}\|} \right) \ (\mathrm{dB}), \tag{2}$$

where $\vec{\rho} = (\rho_1, \rho_2, \ldots, \rho_M)$ is a vector of M samples of the actual output of the FW-LP, and $\vec{e} = (e_1, e_2, \ldots, e_M)$ is a vector of M samples of the difference between the predicted output and the real FW-LP output, i.e., $e_i = \rho_i - f(\vec{x}_i)$, $i = 1, 2, \ldots, M$.

At the antenna level, we employ the following relative error as a figure of merit:

$$\mathrm{RE}_{\mathrm{FF}} = 100 \cdot \frac{\|G_{\text{FW-LP}} - G_{\mathrm{SVR}}\|}{\|G_{\text{FW-LP}}\|} \ (\%), \tag{3}$$

where G is either the copolar or the crosspolar gain pattern, which was obtained either analysing the antenna with a FW-LP (a MoM-LP in the present case [17]) and the real angles of incidence for each element, or estimating (1) with the SVR and a reduced set of angles.

Finally, it is interesting to highlight that in the 4D case, since the angle of incidence is considered an input variable, 10 SVR models are necessary to characterize $\boldsymbol{R}_k, \forall\, k = 1, 2, \ldots, K$. These are the magnitude of two direct coefficients and the real and imaginary parts of the four coefficients. Meanwhile, in the 2D case, each angle of incidence requires ten models, making a total number of $10M_a$ models, where M_a is the number of considered angles of incidence.

C. Penalties of Dimensionality

In light of what is said above, it seems that the 4D case should outperform the 2D case since the latter requires a higher number of surrogate models to characterize all the elements in the reflectarray. Nevertheless, this may not be the case since the number of training samples, N_r, and the training time complexity dependence over N_r might be very different for each procedure. For common training strategies, the time complexity varies between $O\left(N_r^2\right)$ and $O\left(N_r^3\right)$ [18], depending on the value of the hyper-parameters, including the LibSVM library [19], [20] used here. This dependence on the hyper-parameters was verified by experiments in previous works [7, Fig. 4].

The use of angle information as two extra input dimensions of the SVR associates a noticeable growth in the number of training samples to maintain a comparable accuracy to the 2D case. Let us assume that the number of samples is multiplied by factor $M_D > 1$ when producing a 4D SVR model instead of a 2D SVR model. Let us also assume that this factor M_D is similar to the number of considered incidence angles for the 2D case, M_a. Therefore, the computational time to produce the FW-LP samples is approximately the same for both types of SVR. Nevertheless, the computational time required to produce the SVR models does not follow this pattern. The training of the M_a 2D SVR models is proportional to $M_a N_r^2$, in the best case, and to $M_a N_r^3$, in the worst case. Meanwhile, the training of the 4D SVR model is proportional to $M_D^2 N_r^2$, in the best case, and to $M_D^3 N_r^3$, in the worst case. Thus, the time complexity of the 4D SVR is considerably larger than its 2D SVR counterpart, unless $M_D \ll M_a$. This preliminar analysis is corroborated by the numerical results in the following Sections.

D. Discretization of the Angles of Incidence

There are three possibilities to generate the 2D SVR. First, we can generate models only for normal incidence. However, as discussed in Section II-A, this is only suitable for the direct coefficients in (1) due to their good angular stability. Thus, a second method may be to generate models for each reflectarray element, considering the real angle of incidence at each unit cell. This would be the most accurate method at the expense of generating $10K$ models in total. Since reflectarrays are usually comprised of hundreds or even thousands of elements (K), we deem this approach unsuitable. Instead, we consider a third possibility that is a compromise between the previous two. By defining a reduced set of angles of incidence, much smaller than the total number of unit cells in the antenna, the reflectarray elements can be assigned to the closest angle of incidence, thus reducing the total number of (θ, φ) pairs and SVR models.

A study was carried out to select the best discretization of (θ, φ) with the same testing conditions as in [10]. From this study, a few conclusions were drawn. First, although the copolar pattern is robust against the discretization, the crosspolar pattern is not. In fact, when using normal incidence, the error for the copolar pattern is lower than 1.7%, but it is around 80% for the crosspolar pattern. To achieve an overall low error in the prediction of the far field, a proper discretization of θ and φ is required. A uniform discretization with steps of $\Delta\theta = 5°$ and $\Delta\varphi = 10°$ provides an error lower than 1% for the copolar pattern and lower than 10% for the crosspolar pattern. These values guarantee acceptable errors in the prediction of the radiation patterns. For this work, we have chosen a non-uniform discretization in which the selected training angle for θ is given by the set $\{5°, 10°, 17°, 23°, 29°, 35°, 40°\}$ and φ is discretized uniformly in steps of $\Delta\varphi = 10°$, giving a total of 152 (θ, φ) pairs. With this discretization, the error of the copolar pattern is 0.33% and for the crosspolar pattern is 4.58%.

III. Cell Modelling Performance

From here on, we employ the same unit cell and substrate as in [10]. This unit cell is comprised of two sets of parallel dipoles in two layers of metallization and analysed with the MoM-LP of [17].

A. Training Performance

First, we will compare the training performance of the 2D and 4D SVRs. In order to do so, we will split each set of samples into three different subsets as indicated in Section II-B. In addition, we will focus on the time cost and on the accuracy. The latter will be measured in terms of the relative error of the regression over the test set as given by (2). For the 2D SVR, the number of considered angles will be $M_a = 76$, which is halved from 152 pairs using symmetry in φ, and the number of samples per angle will be 2500. Thus, the total amount of samples will be $N = 190\,000$ for the 2D case. Meanwhile, $N = 65\,000$ for the 4D case.

Fig. 2 shows the total training time cost, t_{train}, for both 2D and 4D SVRs against the percentage of training samples (N_r) with respect to the total number of samples, i.e. $N_r/N{\cdot}100$ (%). For the 2D approach, this time cost is the sum of the time costs of the training of every output variable and angle of incidence. For the 4D approach, this time cost is the sum of the time costs of the training of every output variable. As expected, t_{train} increases with N_r for both approaches. Nevertheless, the time cost of the 4D approach is much higher than for the 2D case. Indeed, except for the three left-most points of the curve, the time cost of the 4D training is around 50 times higher.

Fig. 3 plots the average value of the relative test error given by (2) of the direct coefficients magnitude, the real and the imaginary parts

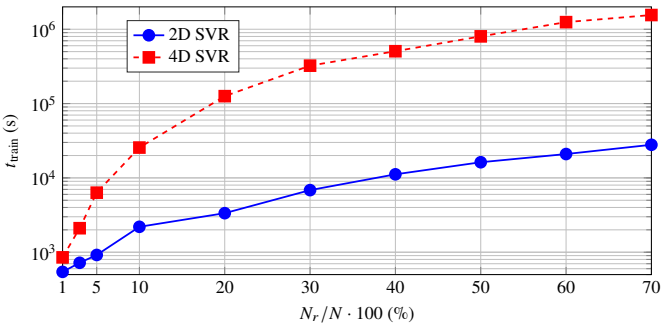

Fig. 2. Total training time, t_{train} (s), vs. the percentage of training patterns with respect to the total number of samples, $N_r/N \cdot 100$ (%), for both the 2D and 4D SVRs. N for 4D SVR is 65 000, while for 2D SVR is 190 000.

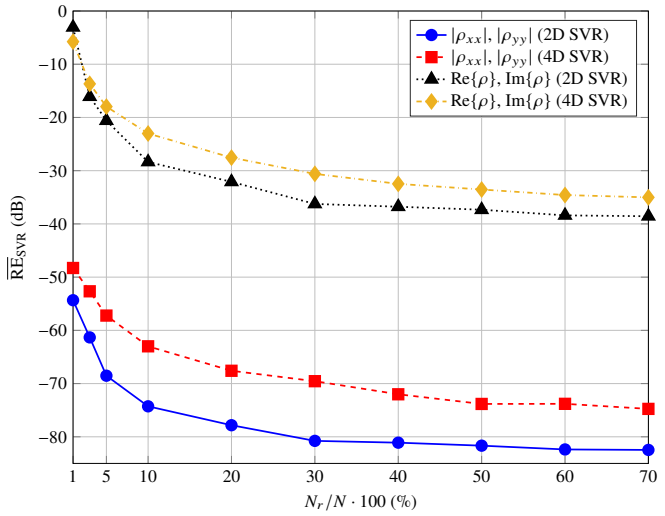

Fig. 3. Average relative test error, $\overline{\text{RE}}_{\text{SVR}}$ (dB), of the reflection coefficients vs. the percentage of training patterns with respect to the total number of samples, $N_r/N \cdot 100$ (%), for both the 2D and 4D SVRs. N for 4D SVR is 65 000, while for 2D SVR is 190 000.

of all the reflection coefficients versus the percentage of training samples. The relative error rapidly decreases with the number of training patterns until the percentage of the samples reaches approximately 30%, where the slope of the relative error starts to approach to zero. This effect is more noticeable in the 2D cases than in the 4D case. In addition, it is more critical the error for the real and imaginary parts of the reflection coefficients, from which their phase is extracted, as well as the magnitude of the cross-coefficients. An average relative error lower than −30 dB ensures a high degree of accuracy between the SVR-based model and the MoM-LP simulations. In light of the above considerations, a good trade-off between training time and relative error may be achieved for $N_r = 0.3N$.

All the results given in this section have been obtained using, in sequential mode, a workstation with 2 Intel Xeon E5-2650v3 CPU at 2.3 GHz and 256 GB of RAM.

B. Reflection Coefficients

The low error achieved in the surrogate model training should materialize in accurate predictions of the reflection coefficients. Fig. 4 shows a comparison between the MoM-LP, 2D SVR and 4D SVR of the magnitude and phase for the direct coefficient ρ_{yy} and for the cross-coefficient ρ_{yx} at oblique incidence $(\theta, \varphi) = (36°, 50°)$ and using $N_r = 0.3N$. As it can be seen, there is a high degree of accuracy for both SVRs when compared with MoM-LP. In fact, for the curves

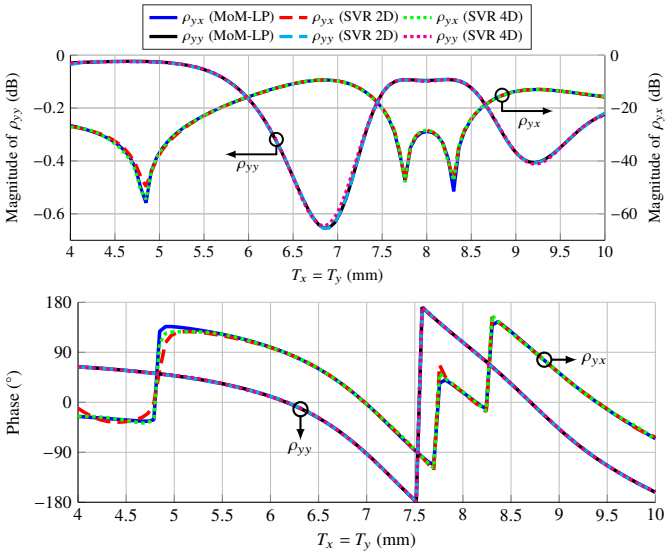

Fig. 4. Comparison between the MoM-LP and SVR simulations of the magnitude (top) and phase (bottom) for the direct reflection coefficient ρ_{yy} and the cross-coefficient ρ_{yx} for oblique incidence $(\theta, \varphi) = (36°, 50°)$.

shown in Fig. 4, the mean absolute deviation (MAD) for the phase of ρ_{yy} is 0.45° and 0.41° for the 2D and 4D SVRs, respectively. Those numbers are 3.81° and 1.93° for the cross-coefficient ρ_{yx}. Regarding the magnitude, the MAD for ρ_{yy} is −77.43 dB and −68.84 dB for the 2D and 4D SVRs, respectively; while for ρ_{yx} they are −56.96 dB and −57.54 dB respectively. Similar results were obtained for the coefficients ρ_{xx} and ρ_{xy} in both magnitude and phase.

The relative error over the test set was calculated for all coefficients for both SVRs using (2). For the 2D SVR it includes the coefficients for all angles of incidence. The average value of the relative error is −40.47 dB for the 2D SVR and −36.94 dB for the 4D SVR.

IV. Radiation Patterns

The most immediate result of the SVR is the accurate prediction of the reflection coefficients in (1). However, the ultimate goal is to use the SVR for the efficient analysis of reflectarrays. This encompasses two aspects: the acceleration with regard to MoM-LP simulations and the accuracy in the prediction of the far field. For this Section, details on the antenna optics are the same as those in [10].

A. Acceleration of Reflectarray Analysis

Fig. 5 shows the acceleration results for the 2D and 4D SVRs for different values of $N_r/N \cdot 100$ (%). It can be observed how the SVR becomes slower when N_r increases. This is expected since the number of support vectors per coefficient increases to obtain a higher accuracy. Nevertheless, for a similar accuracy as the 2D SVR, the 4D SVR is much slower (between 10 and 20 times slower), and even the fastest 4D SVR, with $N_r = 0.01N$, is more than two times slower than the slowest 2D SVR and presents worse accuracy in the prediction of the reflection coefficients than the 2D SVR.

B. Accuracy in the Radiation Pattern Computation

Fig. 6 shows the relative error (3), for both the 2D and 4D SVRs, as a function of the percentage $N_r/N \cdot 100$ (%). It has been obtained with the same large reflectarray with European contoured-beam as in [10]. For all cases, it can be seen that the error rapidly decreases with N_r. For the 4D SVR, the error of the copolar pattern stagnates around 1%, and around 2% for the crosspolar pattern. In contrast, for the 2D

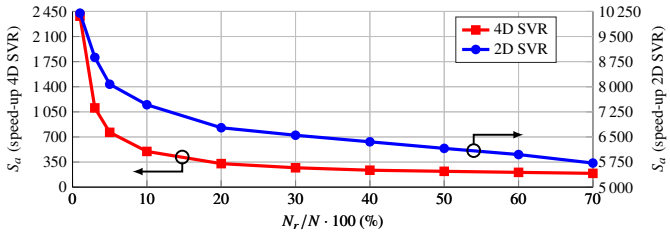

Fig. 5. Reflectarray analysis speed-up (S_a) of the 4D and 2D SVRs for different values of the percentage of training samples.

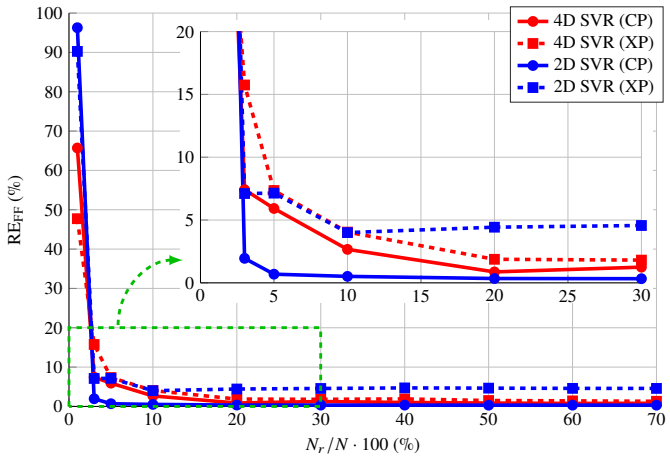

Fig. 6. Relative error in the computation of the far field with the 2D and 4D SVRs for the copolar (CP) and crosspolar (XP) patterns versus the percentage of the training samples.

SVR the relative error for the copolar pattern is more stable and lower, with a value around 0.3%, but the crosspolar pattern presents a relative error around around 4%. It is interesting to note that the error stagnates very quickly when increasing the number of training samples in contrast to the test error shown in Fig. 3. This means that there is a point in which obtaining better accuracy in the prediction of the reflection coefficients does not translate into a lower error in the prediction of the radiation pattern. It is also noteworthy that the test error achieved by the 2D SVR model is lower than the test error for the 4D SVR model (see Fig. 3). This shows the effect of the angles of incidence discretization on the prediction of the radiation pattern, which affects more the crosspolar component than the copolar pattern. Since the 4D SVR includes the angles of incidence as input variables, it does not suffer from this problem. However, the error for the copolar pattern using the 2D SVR is lower.

C. Evaluation of Different Radiation Patterns

Here, we will graphically compare the different approaches. To that end, a dual-linear reflectarray will be designed by following the steps detailed in [10]. Please note that according to Fig. 1, the vertical polarization (V) corresponds to the field aligned to the $\hat{x}_r$ axis. In addition, the following tools will be compared. The MoM-LP will serve as the baseline. Then, attending to the results of Fig. 6, the 4D SVR with $N_r = 0.3N$ and the 2D SVR with $N_r = 0.1N$ will be compared. With these values of N_r, the total number of training samples considering all (θ, φ) pairs is approximately the same (19 500 for the 4D SVR and 19 000 for 2D SVR). This will make the comparison fairer while guaranteeing a low error for the copolar and crosspolar patterns. Table I gathers information about

Table I
SUMMARY OF THE SELECTED SVRS FOR THE FINAL COMPARISON. TIMES WERE MEASURED IN PARALLEL MODE.

SVR	N_r	$t_{\text{gen. pat.}}$ (s)	t_{train} (s)	Speed-up
4D	19 500	132	32 363	271
2D	19 000	128	55	7 462

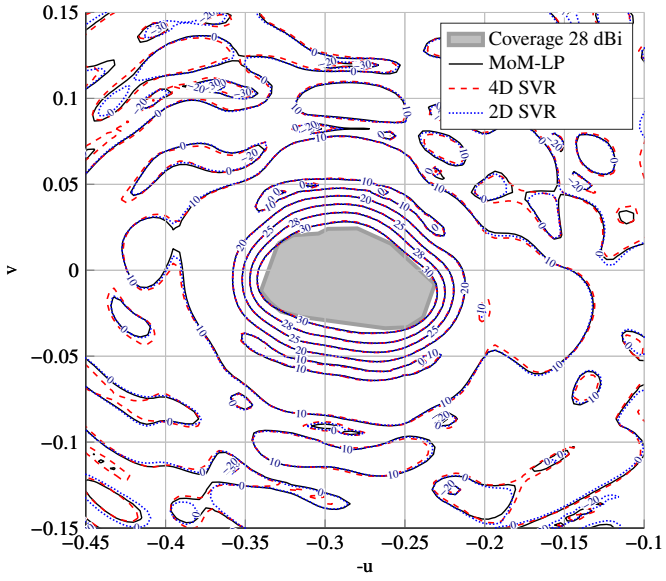

(a)

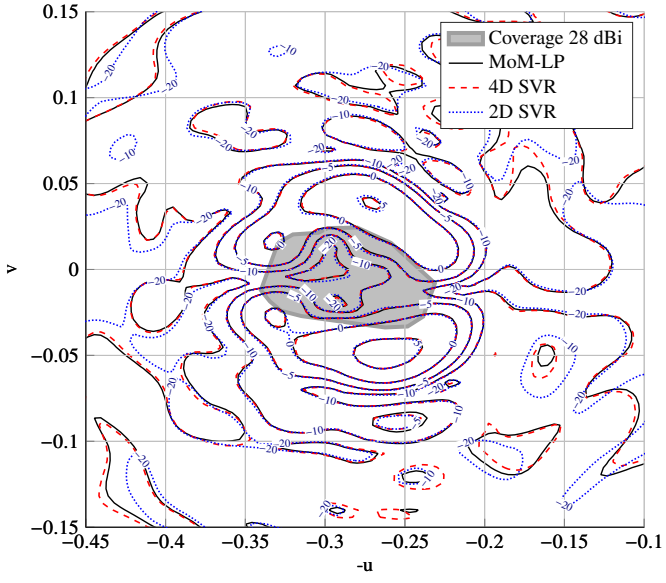

(b)

Fig. 7. Comparison of the MoM-LP simulation and SVR predictions for the (a) copolar and (b) crosspolar patterns for polarization V of a very large reflectarray with European coverage for DTH application.

the selected SVRs. Please note that despite the similar number of training patterns, the 4D SVR training is much slower.

Fig. 7 shows, for polarization V, the radiation pattern for the very large reflectarray with European coverage used for the study of Fig. 6. The accuracy in the prediction of the copolar pattern for both SVR is very high, with very slight discrepancies for the 4D SVR for the

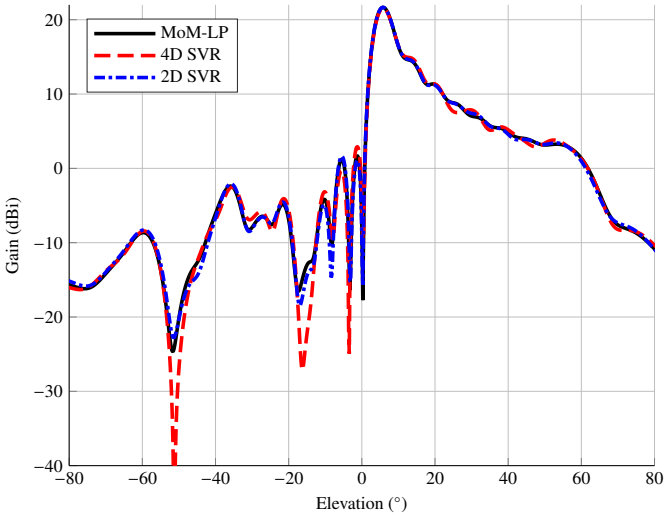

(a)

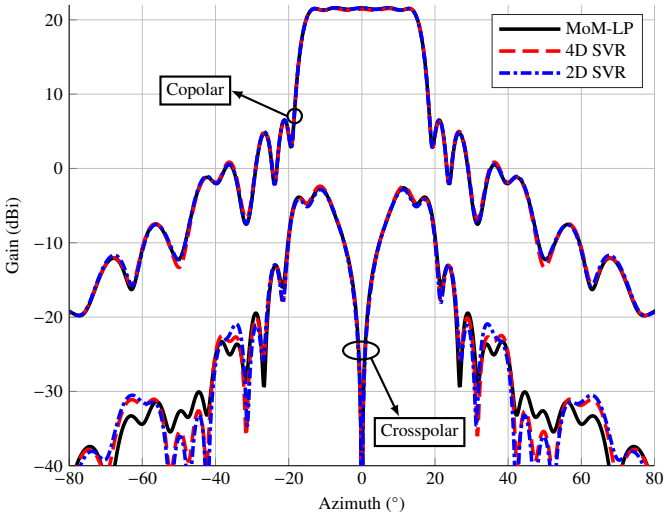

(b)

Fig. 8. Main cuts for the copolar and crosspolar radiation pattern with (a) squared-cosecant pattern in elevation and (b) sectored beam in azimuth for polarization V comparing the MoM-LP and SVR predictions.

10 dBi curves and below. The 4D SVR is only slightly better for the prediction of the crosspolar pattern. The 2D SVR has high accuracy for the high levels of the crosspolar pattern, although presents some minor discrepancies for lower levels.

The comparison has also been carried out with a different radiation pattern than the one employed in the study of Section IV-B: a shaped-beam reflectarray with a sectored beam pattern in azimuth and a squared-cosecant pattern in elevation. This radiation pattern presents a dynamic range in the coverage zone of almost 15 dB in elevation, where the copolar component has to smoothly decrease over an angular span of 50°. Fig. 8 shows the main cuts for this radiation pattern. The copolar component is predicted with a high degree of accuracy by the 2D SVR. The 4D SVR presents deeper nulls as well as slightly higher ripple in the coverage zone of the squared-cosecant beam in elevation. For the crosspolar pattern, both SVRs present similar results and model with high accuracy the region of maximum crosspolar gain, but present some deviation for values lower than −30 dBi (50 dB below peak gain).

Finally, Table II summarizes the errors obtained for the previous patterns, including also a pencil beam. For all examples, similar

Table II
RELATIVE ERRORS (%) IN THE PREDICTION OF THE THREE RADIATION PATTERNS FOR THE COPOLAR (CP) AND CROSSPOLAR (XP) PATTERNS.

Tool	Contoured-beam		Shaped-beam		Pencil beam	
	CP	XP	CP	XP	CP	XP
2D SVR	0.51	4.00	0.91	3.47	0.21	2.14
4D SVR	1.25	1.81	2.08	2.53	0.40	1.01

results were obtained in both linear polarizations. As it can be seen, the 2D SVR model offers lower error in the copolar pattern, although the 4D SVR is slightly better at predicting the crosspolar pattern. In light of these results, it is clear that the 4D SVR, which includes the angles of incidence (θ, φ) as input variables, offers slightly more accuracy in the prediction of the crosspolar pattern than the 2D SVR. However, this higher accuracy is achieved at the expense of greater training time and lower computational efficiency in the analysis of reflectarray antennas. Thus, a compromise might be achieved to greatly accelerate training and analysis time by employing a 2D discretization of the angles of incidence at the expense of slightly decreasing the accuracy of the crosspolar pattern while also maintaining and even increasing the accuracy in the prediction of the copolar pattern.

V. CONCLUSIONS

In this work, we have carried out a study on the use of the angles of incidence in surrogate models based on support vector regression (SVR) for reflectarray design. Two approaches were considered: including the angles of incidence plus two geometrical features of the unit cell as input variables, obtaining a 4D SVR; and grouping different angles of incidence into discrete sets and obtaining 2D SVR models per set. When the 2D and 4D SVRs are compared, the 2D SVR is considerably faster than the 4D SVR. It is between one and two orders of magnitude faster to train and more than one order of magnitude faster to accelerate the reflectarray analysis. Moreover, the copolar pattern presents a higher degree of accuracy with regard to MoM-LP simulations. Only in the prediction of the crosspolar pattern is the 4D SVR slightly more accurate, although both approaches (2D and 4D) achieve errors below 4%. In addition, it has also been shown that there is a point at which obtaining better accuracy in the prediction of the reflection coefficients does not translate into a lower error in the prediction of the radiation pattern.

In contrast to the common approach in the literature, this work has shown that it is more competitive to group the reflectarray elements under a small set of angles of incidence and train surrogate models per each angle of the set, than using the angles of incidence as input variables to the surrogate models. The presented methodology provides faster trainings and reflectarray analyses without significantly compromising the analysis accuracy.

REFERENCES

[1] M. Musseta, P. Pirinoli, P. T. Cong, M. Orefice, and R. E. Zich, "Characterization of microstrip reflectarray square ring elements by means of an Artificial Neural Network," in *Proceedings of the Fourth European Conference on Antennas and Propagation (EuCAP)*, Barcelona, Spain, Apr. 12–16, 2010, pp. 1–4.

[2] P. Robustillo, J. Zapata, J. A. Encinar, and J. Rubio, "ANN characterization of multi-layer reflectarray elements for contoured-beam space antennas in the Ku-band," *IEEE Trans. Antennas Propag.*, vol. 60, no. 7, pp. 3205–3214, Jul. 2012.

[3] A. Freni, M. Mussetta, and P. Pirinoli, "Neural network characterization of reflectarray antennas," *Int. J. Antennas Propag.*, vol. 2012, pp. 1–10, May 2012.

[4] F. Güneş, S. Nesil, and S. Demirel, "Design and analysis of Minkowski reflectarray antenna using 3-D CST Microwave Studio-based neural network model with particle swarm optimization," *Int. J. RF Microw. Comput. Eng.*, vol. 23, no. 2, pp. 272–284, Mar. 2013.

[5] P. Robustillo, J. Zapata, J. A. Encinar, R. Florencio, R. R. Boix, and J. R. Mosig, "Accurate characterization of multi-resonant reflectarray cells by artificial neural networks," in *The 8th European Conference on Antennas and Propagation (EUCAP)*, The Hague, The Netherlands, Apr. 6–11, 2014, pp. 2297–2299.

[6] V. Richard, R. Loison, R. Gillard, H. Legay, and M. Romier, "Loss analysis of a reflectarray cell using ANNs with accurate magnitude prediction," in *11th European Conference on Antennas and Propagation (EuCAP)*, Paris, France, Mar. 19–24, 2017, pp. 2402–2405.

[7] D. R. Prado, J. A. López-Fernández, G. Barquero, M. Arrebola, and F. Las-Heras, "Fast and accurate modeling of dual-polarized reflectarray unit cells using support vector machines," *IEEE Trans. Antennas Propag.*, vol. 66, no. 3, pp. 1258–1270, Mar. 2018.

[8] M. Salucci, L. Tenuti, G. Oliveri, and A. Massa, "Efficient prediction of the EM response of reflectarray antenna elements by an advanced statistical learning method," *IEEE Trans. Antennas Propag.*, vol. 66, no. 8, pp. 3995–4007, Aug. 2018.

[9] J. Huang and J. A. Encinar, *Reflectarray Antennas*. Hoboken, NJ, USA: John Wiley & Sons, 2008.

[10] D. R. Prado, J. A. López-Fernández, M. Arrebola, and G. Goussetis, "Support vector regression to accelerate design and crosspolar optimization of shaped-beam reflectarray antennas for space applications," *IEEE Trans. Antennas Propag.*, vol. 67, pp. 1659–1668, Mar. 2019.

[11] D. R. Prado, M. Arrebola, M. R. Pino, R. Florencio, R. R. Boix, J. A. Encinar, and F. Las-Heras, "Efficient crosspolar optimization of shaped-beam dual-polarized reflectarrays using full-wave analysis for the antenna element characterization," *IEEE Trans. Antennas Propag.*, vol. 65, no. 2, pp. 623–635, Feb. 2017.

[12] D. M. Pozar, S. D. Targonski, and H. D. Syrigos, "Design of millimeter wave microstrip reflectarrays," *IEEE Trans. Antennas Propag.*, vol. 45, no. 2, pp. 287–296, Feb. 1997.

[13] J. A. Encinar, "Design of a dual frequency reflectarray using microstrip stacked patches of variable size," *Electron. Lett.*, vol. 32, no. 12, pp. 1049–1050, Jun. 1996.

[14] M. R. Chaharmir, J. Shaker, and H. Legay, "Broadband design of a single layer large reflectarray using multi cross loop elements," *IEEE Trans. Antennas Propag.*, vol. 57, no. 10, pp. 3363–3366, Oct. 2009.

[15] F. Xue, H.-J. Wang, M. Yi, G. Liu, and X.-C. Dong, "Design of a broadband single-layer linearly polarized reflectarray using four-arm spiral elements," *IEEE Antennas Wireless Propag. Lett.*, vol. 16, pp. 696–699, 2017.

[16] P. Nayeri, F. Yang, and A. Z. Elsherbeni, "Design of single-feed reflectarray antennas with asymmetric multiple beams using the particle swarm optimization method," *IEEE Trans. Antennas Propag.*, vol. 61, no. 9, pp. 4598–4605, Sep. 2013.

[17] R. Florencio, R. R. Boix, and J. A. Encinar, "Enhanced MoM analysis of the scattering by periodic strip gratings in multilayered substrates," *IEEE Trans. Antennas Propag.*, vol. 61, no. 10, pp. 5088–5099, Oct. 2013.

[18] L. Bottou and C.-J. Lin, "Support vector machine solvers," in *Large Scale Kernel Machines*, L. Bottou, O. Chapelle, D. DeCoste, and J. Weston, Eds. Cambridge, MA, USA: MIT Press, 2007, pp. 301–320. [Online]. Available: http://leon.bottou.org/papers/bottou-lin-2006

[19] C.-C. Chang and C.-J. Lin, "LIBSVM: A library for support vector machines," *ACM Trans. Intell. Syst. Technol.*, vol. 2, no. 3, pp. 27:1–27:27, Apr. 2011, software available at https://www.csie.ntu.edu.tw/~cjlin/libsvm.

[20] A. Abdiansah and R. Wardoyo, "Time complexity analysis of support vector machines (SVM) in LibSVM," *Int. J. Comput. Appl.*, vol. 128, no. 3, pp. 28–34, Oct. 2015.